JOURNAL OF AIRCRAFT
Vol. 44, No. 3, May–June 2007

Predicting Maximum Lift Coefficient for Twisted Wings Using Lifting-Line Theory

W. F. Phillips* and N. R. Alley†
Utah State University, Logan, Utah 84322-4130

DOI: 10.2514/1.25640

A method is presented that allows one to predict the maximum lift coefficient for a wing from knowledge of wing geometry and maximum airfoil section lift coefficient. The method applies to wings of arbitrary planform and includes the effects of twist and sweep. In addition to predicting the section lift distribution for a wing of known planform with a known twist distribution, the method can be used to predict the twist distribution, which will produce any desired section lift distribution along the span of an unswept wing of any given planform. The method is shown to predict the twist distribution required to minimize induced drag and is also used to predict the twist distribution that maximizes the wing lift coefficient, while keeping the total amount of required twist at a practical level.

Nomenclature

A_n	=	Fourier coefficients in the series solution to the lifting-line equation
a_n	=	planform contribution to the Fourier coefficients in the series solution to the lifting-line equation
B_n	=	Fourier coefficients in the expansion for $f(\theta)$
b	=	wingspan
b_n	=	twist contribution to the Fourier coefficients in the series solution to the lifting-line equation
C_{Di}	=	wing induced drag coefficient
C_j	=	coefficients in the definition of F_j
C_L	=	wing lift coefficient
$\tilde{C}_L$	=	local airfoil section lift coefficient
$\tilde{C}_{Ld}$	=	local design airfoil section lift coefficient
$C_{L_{\max}}$	=	maximum wing lift coefficient
$\tilde{C}_{L_{\max}}$	=	maximum airfoil section lift coefficient
$C_{L,\alpha}$	=	wing lift slope
$\tilde{C}_{L,\alpha}$	=	airfoil section lift slope
c	=	local airfoil section chord length
c_{root}	=	root airfoil section chord length
F	=	twist-dependent function of θ used to define the normalized twist distribution function
F_j	=	value of F at node j
f	=	lift-dependent function of θ used to define the normalized lift distribution function
f_i	=	value of f at node i
G_i	=	function of θ used to define $F(\theta)$
G_{ij}	=	coefficients in the expansion for F_j
g_k	=	function of θ used to define G_i
g_{kj}	=	value of g_k at node j
i, j, k, n	=	dummy index integers
L	=	airfoil section lift
M	=	number of nodes per semispan
m_t	=	transition index integer
N	=	number of nonzero terms in the truncated Fourier series
q_n	=	Fourier coefficients used to evaluate b_n
R_A	=	wing aspect ratio
R_T	=	wing taper ratio
V_∞	=	magnitude of the freestream velocity
W_{ki}	=	coefficients in the definition for G_i
w_n	=	Fourier coefficients in the expansion for $F(\theta)$
z	=	spanwise coordinate
α	=	geometric angle of attack relative to the freestream
α_{L0}	=	airfoil section zero-lift angle of attack
Γ	=	spanwise section circulation distribution
δ_k	=	spanwise increment used in the definition for W_{ki}
$\delta\theta$	=	spanwise θ increment between nodes
ζ	=	dummy variable
θ	=	change of variables for the spanwise coordinate
θ_i	=	value of θ at node i
$\theta_{\max}$	=	value of θ at the wing section that supports the maximum airfoil section lift coefficient
κ_D	=	planform contribution to the induced drag factor
κ_{DL}	=	lift-twist contribution to the induced drag factor
$\kappa_{D\Omega}$	=	twist contribution to the induced drag factor
κ_{Ls}	=	stall factor in the relation for maximum lift coefficient
$\kappa_{L\Lambda}$	=	sweep factor in the relation for maximum lift coefficient
$\kappa_{L\Omega}$	=	twist factor in the relation for maximum lift coefficient
$\kappa_{\Lambda 1}, \kappa_{\Lambda 2}$	=	sweep coefficients
Λ	=	quarter-chord sweep angle
ϕ_{ki}	=	change of variables used in the definition for W_{ki}
Ω	=	total twist, geometric plus aerodynamic
ω	=	normalized twist distribution function

Introduction

PRANDTL'S classical lifting-line theory [1,2] can be used to obtain an infinite series solution for the spanwise distribution of vorticity generated on a finite wing. If the circulation about any section of the wing is $\Gamma(z)$, where z is measured outboard from the wing root, then Helmholtz's vortex theorem combined with the circulation theory of lift produces the fundamental equation that forms the foundation of Prandtl's lifting-line theory:

$$\frac{2\Gamma(z)}{V_\infty c(z)} + \frac{\tilde{C}_{L,\alpha}}{4\pi V_\infty}\int_{\zeta=-b/2}^{b/2} \frac{1}{z-\zeta}\left(\frac{\mathrm{d}\Gamma}{\mathrm{d}z}\right)_{z=\zeta} \mathrm{d}\zeta = \tilde{C}_{L,\alpha}[\alpha(z) - \alpha_{L0}(z)] \tag{1}$$

Presented as Paper 1267 at the 45th AIAA Aerospace Sciences Meeting and Exhibit, Reno, NV, 8–11 January 2007; received 5 June 2006; revision received 15 September 2006; accepted for publication 22 September 2006.

*Professor, Mechanical and Aerospace Engineering Department, 4130 Old Main Hill. Member AIAA.

†Graduate Student, Mechanical and Aerospace Engineering Department, 4130 Old Main Hill. Student Member AIAA.

In Eq. (1), α and α_{L0} are allowed to vary with the spanwise coordinate, to account for geometric and aerodynamic twist. For a given wing design, at a given angle of attack and airspeed, the planform shape, airfoil section lift slope, geometric angle of attack, and zero-lift angle of attack are all known functions of spanwise position. The only unknown in Eq. (1) is $\Gamma(z)$.

An analytical solution to Prandtl's lifting-line equation can be obtained in terms of a Fourier sine series. From this solution, the circulation distribution is given by

$$\Gamma(\theta) = 2bV_\infty \sum_{n=1}^{\infty} A_n \sin(n\theta) \tag{2}$$

where

$$\theta \equiv \cos^{-1}(-2z/b) \tag{3}$$

and the Fourier coefficients A_n must satisfy the relation

$$\sum_{n=1}^{\infty} A_n \left[\frac{4b}{\tilde{C}_{L,\alpha} c(\theta)} + \frac{n}{\sin(\theta)} \right] \sin(n\theta) = \alpha(\theta) - \alpha_{L0}(\theta) \tag{4}$$

From this circulation distribution, the resulting lift and induced drag coefficients for the finite wing are found to be

$$C_L = \pi R_A A_1 \tag{5}$$

and

$$C_{Di} = \pi R_A \sum_{n=1}^{\infty} n A_n^2 = \frac{C_L^2}{\pi R_A} + \pi R_A \sum_{n=2}^{\infty} n A_n^2 \tag{6}$$

Methods for evaluating the Fourier coefficients from Eq. (4) are varied and well known [3–6]. For a detailed presentation of Prandtl's lifting-line theory, see Anderson [7], Bertin [8], Katz and Plotkin [9], Kuethe and Chow [10], McCormick [11], or Phillips [12].

The classical lifting-line solution expressed in the form of Eqs. (2–6) is cumbersome for evaluating traditional wing properties for a wing with geometric and/or aerodynamic twist. This is because the aerodynamic angle of attack, $\alpha - \alpha_{L0}$, is not constant along the span of the wing, and the Fourier coefficients A_n change with the operating conditions. Because geometric and aerodynamic twist enter into the lifting-line formulation only as a sum, we need not distinguish between these two types of twist. Hereafter, the word *twist* is used to indicate a spanwise variation in either the local geometric angle of attack or the local zero-lift angle of attack. Twist is treated as positive at those sections having a lower aerodynamic angle of attack than the root and negative at those sections with a higher aerodynamic angle of attack than the root (i.e., washout is defined to be positive twist).

The procedure traditionally used for lifting-line analysis of twisted wings is based on Eqs. (2–6) and requires evaluating separate sets of the Fourier coefficients A_n for more than one angle of attack. Because the lift coefficient predicted from lifting-line theory is a linear function of the angle of attack, the wing lift slope and zero-lift angle of attack for a finite twisted wing can be determined by evaluating only two sets of the Fourier coefficients A_n: one set for each of two different angles of attack. However, as pointed out by Karamcheti [6], the induced drag coefficient for a twisted wing is not a linear function of the lift coefficient squared, as it is for an untwisted wing. Thus, to obtain the induced drag polar for a twisted wing using this procedure, several sets of the Fourier coefficients A_n must be determined over a range of angles of attack. Bertin [8] and Kuethe and Chow [10] present the details of this procedure, together with example computations.

Glauert [3] authored the first textbook to present a lifting-line analysis for twisted wings. In this work, he considered only the rectangular planform with a linear spanwise symmetric variation in twist. In the 1930s and 1940s, this type of analysis became quite commonplace (see, for example, Glauert and Gates [13], Amstutz [14], Anderson [15,16], Datwiler [17], Cohen [18], Falkner [19], DeYoung and Harper [20], and Stevens [21]). In addition to modeling a continuous variation in twist along the span of a finite wing, lifting-line theory has also been used to evaluate the spanwise lift distribution that results from a step change in aerodynamic angle of attack, which is caused by the deflection of partial span trailing-edge flaps and ailerons (Munk [22,23], Glauert [24], Hartshorn [25], Pearson [26,27], and Pearson and Jones [28]). Because a fairly large number of terms must be carried to adequately represent the Fourier expansion of a step function, lifting-line analysis for wings with deflected flaps and ailerons was extremely laborious before the development of the digital computer. This labor was amplified by the fact that the procedure required evaluating a complete set of Fourier coefficients for each angle of attack and flap deflection angle investigated.

Recently, a more practical form of the lifting-line solution for twisted wings has been developed [29–31]. This solution is obtained by using the simple change of variables

$$\alpha(\theta) - \alpha_{L0}(\theta) \equiv (\alpha - \alpha_{L0})_{\text{root}} - \Omega\omega(\theta) \tag{7}$$

where Ω is evaluated at some spanwise reference position

$$\Omega \equiv (\alpha - \alpha_{L0})_{\text{root}} - (\alpha - \alpha_{L0})_{\text{ref}} \tag{8}$$

and $\omega(\theta)$ is the twist distribution normalized with respect to this same reference twist

$$\omega(\theta) \equiv \frac{\alpha(\theta) - \alpha_{L0}(\theta) - (\alpha - \alpha_{L0})_{\text{root}}}{(\alpha - \alpha_{L0})_{\text{ref}} - (\alpha - \alpha_{L0})_{\text{root}}} \tag{9}$$

The normalized twist distribution function is independent of the angle of attack and varies from 0.0 at the root to 1.0 at the reference point, which is commonly taken to be the wingtips. Using Eq. (7) in Eq. (4) gives

$$\sum_{n=1}^{\infty} A_n \left[\frac{4b}{\tilde{C}_{L,\alpha} c(\theta)} + \frac{n}{\sin(\theta)} \right] \sin(n\theta) = (\alpha - \alpha_{L0})_{\text{root}} - \Omega\omega(\theta) \tag{10}$$

The Fourier coefficients A_n in Eq. (10) are written as

$$A_n \equiv a_n(\alpha - \alpha_{L0})_{\text{root}} - b_n\Omega \tag{11}$$

where the Fourier coefficients a_n and b_n are obtained from

$$\sum_{n=1}^{\infty} a_n \left[\frac{4b}{\tilde{C}_{L,\alpha} c(\theta)} + \frac{n}{\sin(\theta)} \right] \sin(n\theta) = 1 \tag{12}$$

and

$$\sum_{n=1}^{\infty} b_n \left[\frac{4b}{\tilde{C}_{L,\alpha} c(\theta)} + \frac{n}{\sin(\theta)} \right] \sin(n\theta) = \omega(\theta) \tag{13}$$

Solutions to Eqs. (12) and (13) are obtained using the same techniques that are commonly used to obtain solutions to Eq. (4). However, solutions to Eqs. (12) and (13) are independent of the angle of attack.

Using Eq. (11) in Eq. (5), the lift coefficient for a twisted wing is given by

$$C_L = \pi R_A [a_1(\alpha - \alpha_{L0})_{\text{root}} - b_1\Omega] \tag{14}$$

Similarly, using Eq. (11) in Eq. (6), the induced drag coefficient for a twisted wing can be expressed as [29]

$$C_{Di} = \frac{C_L^2(1 + \kappa_D) - \kappa_{DL} C_L C_{L,\alpha}\Omega + \kappa_{D\Omega}(C_{L,\alpha}\Omega)^2}{\pi R_A} \tag{15}$$

where

$$C_{L,\alpha} = \pi R_A a_1 \tag{16}$$

$$\kappa_D = \sum_{n=2}^{\infty} n \frac{a_n^2}{a_1^2} \tag{17}$$

$$\kappa_{DL} = 2\frac{b_1}{a_1}\sum_{n=2}^{\infty} n \frac{a_n}{a_1}\left(\frac{b_n}{b_1} - \frac{a_n}{a_1}\right) \tag{18}$$

$$\kappa_{D\Omega} = \left(\frac{b_1}{a_1}\right)^2 \sum_{n=2}^{\infty} n\left(\frac{b_n}{b_1} - \frac{a_n}{a_1}\right)^2 \tag{19}$$

From Eqs. (15–19), it has been shown [29] that minimum possible induced drag always results when the twist distribution is given by

$$\omega(\theta) = 1 - \frac{\sin(\theta)}{c(\theta)/c_{\text{root}}} \tag{20}$$

and the total amount of twist is related to the lift coefficient, according to the relation

$$\Omega = \frac{\kappa_{DL} C_L}{2\kappa_{D\Omega} C_{L,\alpha}} \tag{21}$$

When an unswept wing of arbitrary planform has the twist distribution specified by Eq. (20) and the total amount of twist adjusted, according to Eq. (21), an unswept wing of any planform shape can be designed to operate at a given lift coefficient with the same minimum induced drag as that produced by an untwisted elliptic wing with the same aspect ratio and lift coefficient. This optimum spanwise twist distribution produces an elliptic spanwise lift distribution, which always results in minimum possible induced drag. For a detailed presentation of this solution to Prandtl's lifting-line equation, including several worked example problems, see Phillips [12].

Maximum Section Lift Coefficient

Because, in general, the local section lift coefficient is not constant along the span of a finite wing, it is of interest to know the value of the maximum section lift coefficient and the position along the span at which this maximum occurs [32–38]. Such knowledge allows us to predict the onset of wing stall from known airfoil section properties, including the maximum airfoil section lift coefficient.

From Eq. (2) combined with the vortex lifting law [39], the spanwise variation in local section lift is given by

$$\tilde{L}(\theta) = \rho V_\infty \Gamma(\theta) = 2b\rho V_\infty^2 \sum_{n=1}^{\infty} A_n \sin(n\theta) \tag{22}$$

and the spanwise variation in local section lift coefficient is

$$\tilde{C}_L(\theta) \equiv \frac{\tilde{L}(\theta)}{\frac{1}{2}\rho V_\infty^2 c(\theta)} = \frac{4b}{c(\theta)} \sum_{n=1}^{\infty} A_n \sin(n\theta) \tag{23}$$

The Fourier coefficients A_n in Eq. (23) can be conveniently written using the change of variables given by Eq. (11). Furthermore, solving Eq. (14) for the root aerodynamic angle of attack gives

$$(\alpha - \alpha_{L0})_{\text{root}} = \frac{b_1}{a_1}\Omega + \frac{C_L}{\pi R_A a_1} \tag{24}$$

Using Eq. (24) in Eq. (11) yields

$$A_n = \left(\frac{b_1 a_n}{a_1} - b_n\right)\Omega + \frac{a_n}{\pi R_A a_1} C_L \tag{25}$$

Using this change of variables, Eq. (23) can be written as

$$\tilde{C}_L(\theta) = \Omega \sum_{n=1}^{\infty} 4\left(\frac{b_1 a_n}{a_1} - b_n\right)\frac{\sin(n\theta)}{c(\theta)/b} + C_L \sum_{n=1}^{\infty} \frac{4a_n}{\pi R_A a_1}\frac{\sin(n\theta)}{c(\theta)/b} \tag{26}$$

We see from Eq. (26) that the spanwise variation in local section lift coefficient can be divided conveniently into two components. The first term on the right-hand side of Eq. (26) is called the basic section lift coefficient and the second term is called the additional section lift coefficient. The basic section lift coefficient is independent of C_L and directly proportional to the total amount of wing twist. The additional section lift coefficient at any section of the wing is independent of wing twist and directly proportional to the net wing lift coefficient.

As can be seen from Eq. (26), the basic section lift coefficient is the spanwise variation in local section lift coefficient that occurs when the total net lift developed by the wing is zero. Examination of the first term on the right-hand side of Eq. (26) reveals that the basic section lift coefficient depends on all of the Fourier coefficients a_n and b_n. From Eq. (12), we see that the Fourier coefficients a_n depend only on the wing planform. Equation (13) shows that the Fourier coefficients b_n depend on both the wing planform and $\omega(\theta)$. Thus, the spanwise variation in the basic section lift coefficient depends on wing planform and wing twist but is independent of the wing angle of attack.

Examination of the second term on the right-hand side of Eq. (26) discloses that the additional section lift coefficient depends only on the wing planform and the Fourier coefficients a_n. From Eq. (12), we have seen that the a_n coefficients do not depend on wing twist. Thus, Eq. (26) exposes the important fact that the additional section lift coefficient is independent of wing twist. Because the basic section lift coefficient is zero for an untwisted wing, we see that the additional section lift coefficient is equivalent to the spanwise variation in local section lift coefficient that would be developed on an untwisted wing of the same planform operating at the same wing lift coefficient.

Figure 1 shows how the net section lift coefficient and its two components from Eq. (26) vary along the span of a linearly tapered wing of aspect ratio 8.0 and taper ratio 0.5. This figure shows the spanwise variation in section lift coefficient for several values of total linear twist, with the net wing lift coefficient held constant at 1.0. Similar results are shown in Fig. 2 for three different values of the net wing lift coefficient, with the total linear twist held constant at 6 deg.

Notice that the spanwise coordinates of the maximums in both the basic and additional section lift coefficients do not change with either the amount of wing twist or the net wing lift coefficient. Because the additional section lift coefficient is independent of wing twist, the spanwise position of the aerodynamic center of each wing semispan is not affected by wing twist. However, the maximum in the net section lift coefficient moves inboard as the total amount of twist is increased, and for wings with positive twist (i.e., washout), this

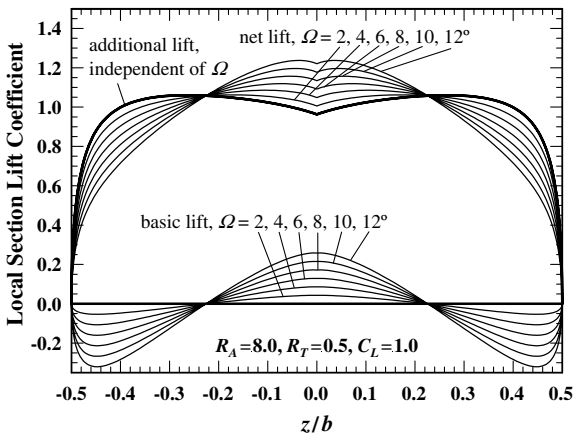

Fig. 1 Spanwise variation in local section lift coefficient as a function of the total amount of linear twist with the net wing lift coefficient held constant at $C_L = 1.0$.

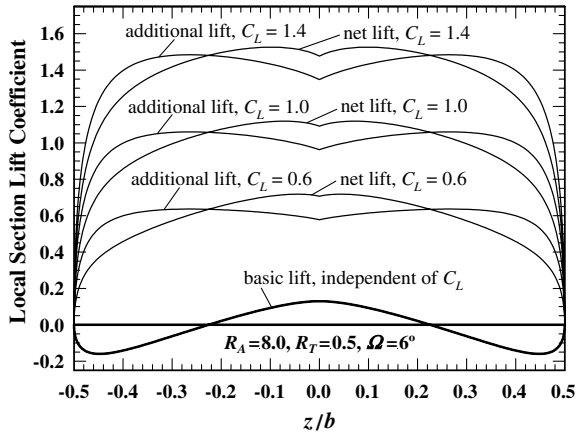

Fig. 2 Spanwise variation in local section lift coefficient as a function of the net wing lift coefficient with the total amount of linear twist held constant at $\Omega = 6$ deg.

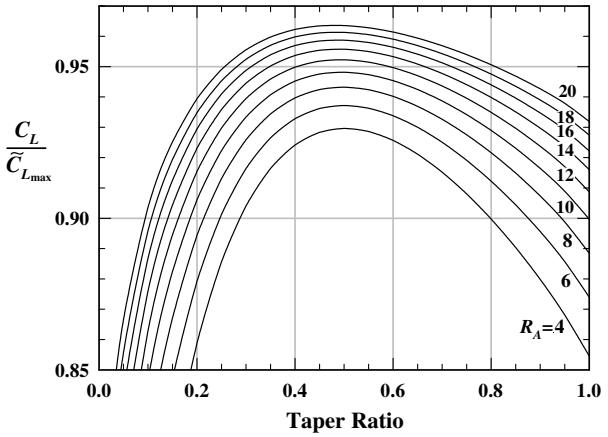

Fig. 3 Maximum lift coefficient for tapered wings with no sweep or twist.

maximum moves outboard as the wing lift coefficient increases. Thus, the spanwise position of the center of pressure on each semispan of a twisted wing varies with both wing twist and angle of attack.

Combining terms from the basic and additional section lift coefficients in Eq. (26) and rearranging, we see that the maximum section lift coefficient occurs at a value of θ that satisfies the relation

$$\frac{\mathrm{d}\tilde{C}_L}{\mathrm{d}\theta} = \frac{4C_L}{\pi R_A}\sum_{n=1}^{\infty}\left(\frac{a_n}{a_1} + \frac{b_1a_n - a_1b_n}{a_1^2}\frac{\pi R_A a_1 \Omega}{C_L}\right) \times \left[b\frac{n\cos(n\theta)c(\theta) - \sin(n\theta)\,\mathrm{d}c/\mathrm{d}\theta}{c^2(\theta)}\right] = 0 \tag{27}$$

In view of Eq. (16), the spanwise location of the airfoil section that supports the largest section lift coefficient is found to be a root of the equation

$$\sum_{n=1}^{\infty}\left(a_n + \frac{b_1a_n - a_1b_n}{a_1}\frac{C_{L,\alpha}\Omega}{C_L}\right) \times \left[n\cos(n\theta)\frac{c(\theta)}{b} - \sin(n\theta)\frac{\mathrm{d}(c/b)}{\mathrm{d}\theta}\right] = 0 \tag{28}$$

In the most general case, this root must be found numerically.

After finding the root of Eq. (28) to obtain the value of θ, which corresponds to the airfoil section that supports the maximum section lift coefficient, this value of θ can be used in Eq. (26) to determine the maximum section lift coefficient for the wing at the specified operating condition. Dividing Eq. (26) by the net wing lift coefficient and applying Eq. (16), the ratio of the local section lift coefficient to the total lift coefficient for the wing can be written as

$$\frac{\tilde{C}_L(\theta)}{C_L} = \frac{4b}{\pi R_A c(\theta)}\left[\sum_{n=1}^{\infty}\frac{a_n}{a_1}\sin(n\theta) + \frac{C_{L,\alpha}\Omega}{C_L}\sum_{n=2}^{\infty}\frac{b_1a_n - a_1b_n}{a_1^2}\sin(n\theta)\right] \tag{29}$$

Examination of Eqs. (28) and (29) reveals that, for $\Omega = 0$, these equations are independent of the net wing lift coefficient. This means that, for an untwisted wing of any planform, the ratio of the maximum section lift coefficient to the total wing lift coefficient and the position along the span at which this maximum occurs are independent of operating conditions and functions of the wing planform only. Figure 3 shows how the ratio of total wing lift coefficient to maximum section lift coefficient varies with aspect ratio and taper ratio for untwisted wings with linear taper.

The spanwise coordinate of the maximum section lift coefficient for such untwisted wings is presented in Fig. 4 as a function of aspect

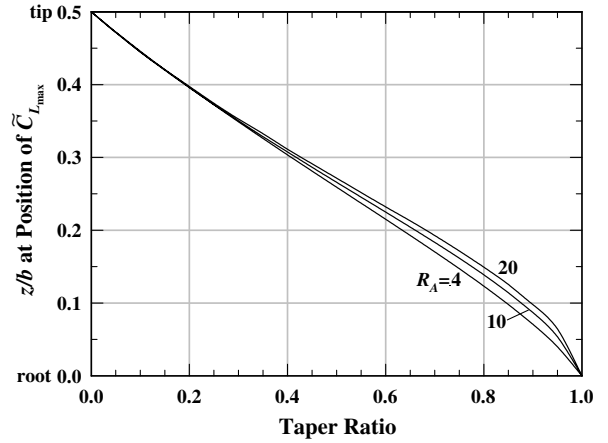

Fig. 4 Spanwise location of maximum section lift coefficient for tapered wings with no sweep or twist.

ratio and taper ratio. Notice that the spanwise coordinate of the airfoil section that supports the maximum section lift coefficient is quite insensitive to the aspect ratio and nearly a linear function of taper ratio.

For elliptic wings with washout, the maximum section lift coefficient always occurs at the wing root, $\theta = \pi/2$; the wing section chord length is given by $c(\theta) = [4b/(\pi R_A)]\sin(\theta)$; and the planform Fourier coefficients are $a_1 = \tilde{C}_{L,\alpha}/(\pi R_A + \tilde{C}_{L,\alpha})$ and $a_n = 0$ for $n > 1$. Using these results in Eq. (29) yields

$$\frac{\tilde{C}_{L_{max}}}{C_L} = 1 + \kappa_{L\Omega}\frac{C_{L,\alpha}\Omega}{C_L} = 1 + \kappa_{L\Omega}\frac{C_{L,\alpha}\Omega}{\tilde{C}_{L_{max}}}\frac{\tilde{C}_{L_{max}}}{C_L} \tag{30}$$

where

$$\kappa_{L\Omega} = \frac{\pi R_A + \tilde{C}_{L,\alpha}}{\tilde{C}_{L,\alpha}}\sum_{n=2}^{\infty} -b_n\sin(n\pi/2) = \frac{\pi R_A + \tilde{C}_{L,\alpha}}{\tilde{C}_{L,\alpha}}\sum_{i=1}^{\infty}(-1)^{i+1}b_{2i+1} \tag{31}$$

Equation (30) is readily rearranged to give

$$\frac{C_L}{\tilde{C}_{L_{max}}} = 1 - \kappa_{L\Omega}\frac{C_{L,\alpha}\Omega}{\tilde{C}_{L_{max}}}1 \tag{32}$$

Because $\kappa_{L\Omega}$ is independent of both Ω and C_L for elliptic wings with washout, the ratio $C_L/\tilde{C}_{L_{max}}$ is a linear function of $C_{L,\alpha}\Omega/\tilde{C}_{L_{max}}$. For elliptic wings with linear twist, the coefficients b_n are given by

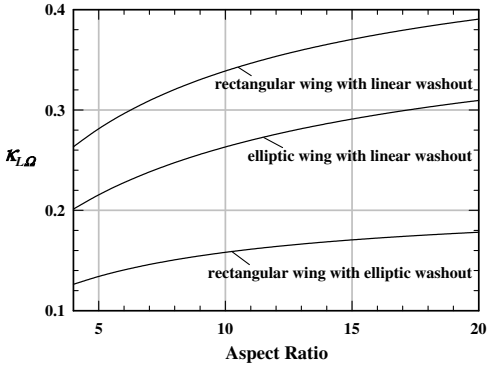

Fig. 5 Effect of wing twist on $\kappa_{L\Omega}$ for elliptic and rectangular wings.

$$b_n = \frac{1}{\pi}\left(\frac{\tilde{C}_{L,\alpha}}{\pi R_A + n\tilde{C}_{L,\alpha}}\right)\begin{cases}\dfrac{4\sin(n\pi/2)}{4-n^2}, & n \neq 2\\ 0, & n = 2\end{cases} \tag{33}$$

Using Eq. (33) in Eq. (31) gives the twist factor that can be used in Eq. (32) to estimate the maximum lift coefficient for elliptic wings with linear washout:

$$\kappa_{L\Omega} = \frac{1}{\pi}\sum_{i=1}^{\infty}\frac{4}{(2i+1)^2-4}\left(\frac{\pi R_A + \tilde{C}_{L,\alpha}}{\pi R_A + (2i+1)\tilde{C}_{L,\alpha}}\right) \tag{34}$$

For a detailed development of Eq. (33), see Phillips [29]. Results predicted from Eq. (34) for elliptic wings with linear washout are shown in Fig. 5 as a function of aspect ratio.

For rectangular wings with washout, the maximum section lift coefficient also occurs at the wing root, $\theta = \pi/2$, and the chord length is given by $c(\theta) = b/R_A$. Using these results in Eq. (29) yields

$$\frac{C_L}{\tilde{C}_{L_{\max}}} = \left(\frac{C_L}{\tilde{C}_{L_{\max}}}\right)_{\Omega=0}\left(1 - \kappa_{L\Omega}\frac{C_{L,\alpha}\Omega}{\tilde{C}_{L_{\max}}}\right) \tag{35}$$

where

$$\left(\frac{C_L}{\tilde{C}_{L_{\max}}}\right)_{\Omega=0} = \frac{\pi}{4}\Bigg/\left[1 + \sum_{i=1}^{\infty}(-1)^i\frac{a_{2i+1}}{a_1}\right] \tag{36}$$

and

$$\kappa_{L\Omega} \equiv \frac{4}{\pi}\sum_{i=1}^{\infty}(-1)^i\frac{b_1 a_{2i+1} - a_1 b_{2i+1}}{a_1^2} \tag{37}$$

Here again, $\kappa_{L\Omega}$ is independent of both Ω and C_L, and the ratio of wing lift coefficient to maximum section lift coefficient is a linear function of $C_{L,\alpha}\Omega/\tilde{C}_{L_{\max}}$. Figure 5 shows how $\kappa_{L\Omega}$ varies with aspect ratio for rectangular wings with both linear and elliptic washout.

Equations (32) and (35) are identical, because for elliptic wings, $(C_L/\tilde{C}_{L_{\max}})_{\Omega=0} = 1$. Equation (35) is readily rearranged to obtain the net wing lift coefficient as a function of the maximum airfoil section lift coefficient and the wing twist. This gives

$$C_L = \left(\frac{C_L}{\tilde{C}_{L_{\max}}}\right)_{\Omega=0}(\tilde{C}_{L_{\max}} - \kappa_{L\Omega}C_{L,\alpha}\Omega) \tag{38}$$

Equation (38) can be used in combination with the results plotted in Figs. 3 and 5 to estimate the wing lift coefficient at the onset of airfoil section stall. For example, consider a rectangular wing of aspect ratio 8.0 with 4.0 deg (0.0698 rad) of linear washout and a maximum airfoil section lift coefficient of 1.6. For this wing geometry, $C_{L,\alpha} = 4.838$, $(C_L/\tilde{C}_{L_{\max}})_{\Omega=0} = 0.888$, $\kappa_{L\Omega} = 0.321$, and

$$C_L = \left(\frac{C_L}{\tilde{C}_{L_{\max}}}\right)_{\Omega=0}(\tilde{C}_{L_{\max}} - \kappa_{L\Omega}C_{L,\alpha}\Omega) = 0.888(1.6 - 0.321 \times 4.838 \times 0.0698) = 1.325$$

As was seen in Figs. 1 and 2, for wings of arbitrary planform, the maximum section lift coefficient does not necessarily occur at the root. In general, from Eq. (29), we have

$$\frac{C_L}{\tilde{C}_{L_{\max}}} = \left[\frac{\pi R_A c(\theta_{\max})}{4b}\Bigg/\sum_{n=1}^{\infty}\frac{a_n}{a_1}\sin(n\theta_{\max})\right] \times \left[1 - \frac{C_{L,\alpha}\Omega}{\tilde{C}_{L_{\max}}}\frac{4b}{\pi R_A c(\theta_{\max})}\sum_{n=2}^{\infty}\frac{b_1 a_n - a_1 b_n}{a_1^2}\sin(n\theta_{\max})\right] \tag{39}$$

where $\theta_{\max}$ is the value of θ at the wing section that supports the maximum airfoil section lift coefficient, as obtained from the root of Eq. (28). For an arbitrary planform, Eq. (39) is not always linear in $C_{L,\alpha}\Omega/\tilde{C}_{L_{\max}}$, because, in general, $\theta_{\max}$ depends on $C_{L,\alpha}\Omega/C_L$. However, we can still define the wing parameter $\kappa_{L\Omega}$ to satisfy Eq. (35), but, in general, this parameter will vary with $C_{L,\alpha}\Omega/\tilde{C}_{L_{\max}}$ as well as with the wing planform. The results plotted in Figs. 6 and 7 show how $\kappa_{L\Omega}$ varies with $C_{L,\alpha}\Omega/\tilde{C}_{L_{\max}}$ for wings with linear taper and linear washout. Notice that $\kappa_{L\Omega}$ is independent of $C_{L,\alpha}\Omega/\tilde{C}_{L_{\max}}$ only for a taper ratio of 1.0.

Equation (38) can be used in combination with the results plotted in Figs. 3, 6, and 7 to estimate the wing lift coefficient at the onset of airfoil section stall for tapered wings with linear washout. For example, consider a tapered wing of aspect ratio 8.0 and taper ratio 0.5 with 4.0 deg of linear washout and a maximum airfoil section lift coefficient of 1.6. For this geometry, $C_{L,\alpha} = 4.964$, $(C_L/\tilde{C}_{L_{\max}})_{\Omega=0} = 0.943$, and $C_{L,\alpha}\Omega/\tilde{C}_{L_{\max}} = 0.217$, which yields $\kappa_{L\Omega} = 0.034$. Using

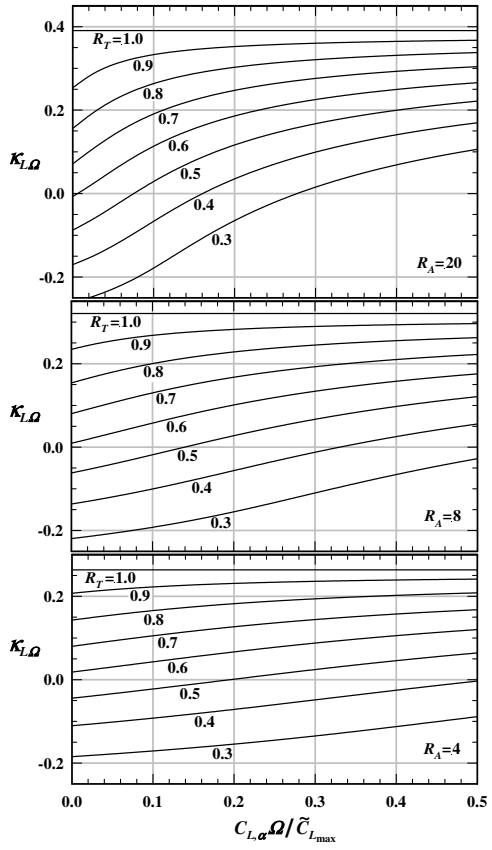

Fig. 6 Effect of twist and taper ratio on $\kappa_{L\Omega}$ for wings with linear taper and linear washout.

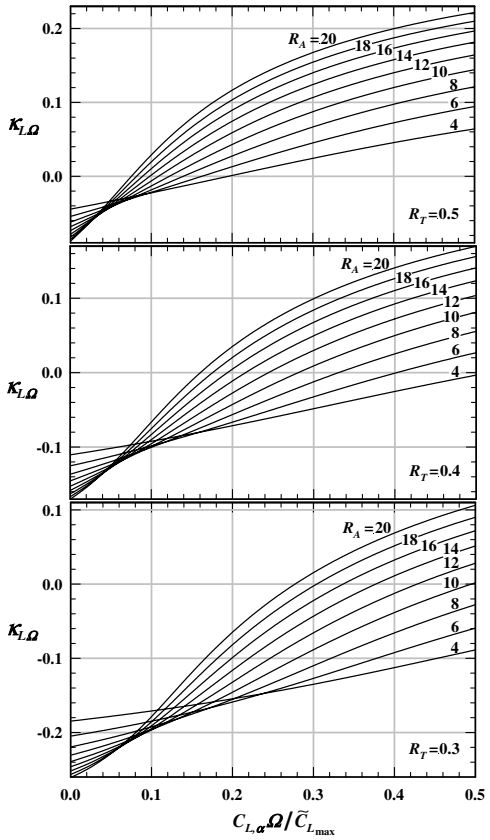

Fig. 7 Effect of twist and aspect ratio on $\kappa_{L\Omega}$ for wings with linear taper and linear washout.

these values in Eq. (38), the total wing lift coefficient at the onset of airfoil section stall is found to be

$$C_L = \left(\frac{C_L}{\tilde{C}_{L_{\max}}}\right)_{\Omega=0} (\tilde{C}_{L_{\max}} - \kappa_{L\Omega} C_{L,\alpha}\Omega) = 0.943(1.6 - 0.034 \times 4.964 \times 0.0698) = 1.498$$

Plotting results such as those shown in Figs. 6 and 7 is easily accomplished by using the unknown parameter $C_{L,\alpha}\Omega/C_L$ as the independent variable. From a specified value of $C_{L,\alpha}\Omega/C_L$, the spanwise location $\theta_{\max}$ of the airfoil section that supports the maximum section lift coefficient is found from the root of Eq. (28). This value for $\theta_{\max}$ is then used in Eq. (29) to evaluate $C_L/\tilde{C}_{L_{\max}}$. Similarly, the ratio $(C_L/\tilde{C}_{L_{\max}})_{\Omega=0}$ is obtained by using $C_{L,\alpha}\Omega/C_L = 0$. With the ratios $C_L/\tilde{C}_{L_{\max}}$ and $(C_L/\tilde{C}_{L_{\max}})_{\Omega=0}$ known, the value of the dependent variable $C_{L,\alpha}\Omega/\tilde{C}_{L_{\max}}$ is obtained from the relation

$$\frac{C_{L,\alpha}\Omega}{\tilde{C}_{L_{\max}}} = \frac{C_{L,\alpha}\Omega}{C_L}\frac{C_L}{\tilde{C}_{L_{\max}}} \tag{40}$$

and $\kappa_{L\Omega}$ is evaluated by rearranging Eq. (35):

$$\kappa_{L\Omega} = \left[1 - \frac{C_L}{\tilde{C}_{L_{\max}}} \Big/ \left(\frac{C_L}{\tilde{C}_{L_{\max}}}\right)_{\Omega=0}\right] \Big/ \frac{C_{L,\alpha}\Omega}{\tilde{C}_{L_{\max}}} \tag{41}$$

The dependent variable obtained from Eq. (41) can be plotted against the dependent variable obtained from Eq. (40) to produce results similar to Figs. 6 and 7 for any spanwise variation in section chord length and wing twist.

For the special case of an unswept wing with the twist optimized to produce minimum induced drag, the twist distribution function is given by Eq. (20) and the total amount of twist is given by Eq. (21). For wings twisted in this manner, the twist is maintained in proportion to the lift coefficient, according to the relation

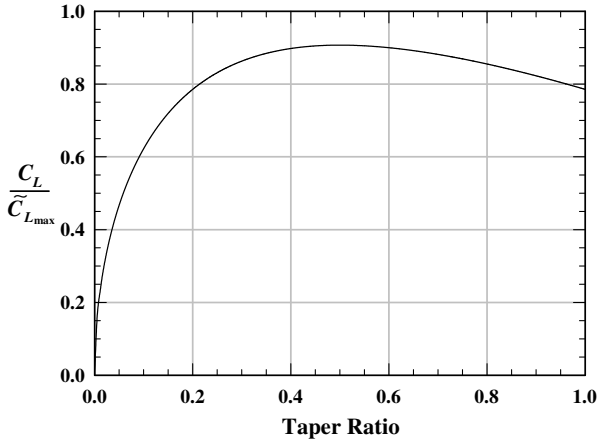

Fig. 8 Maximum lift coefficient for unswept wings with linear taper and the twist optimized to produce minimum induced drag.

$$\Omega = \frac{\kappa_{DL} C_L}{2\kappa_{D\Omega} C_{L,\alpha}} = \frac{\kappa_{DL} C_L}{2\kappa_{D\Omega}\pi R_A a_1} \tag{42}$$

where κ_{DL} and $\kappa_{D\Omega}$ are evaluated from Eqs. (18) and (19), respectively. Using Eq. (42) in Eq. (25) gives

$$A_n = \left(\frac{a_n}{\pi R_A a_1} + \frac{\kappa_{DL}}{2\kappa_{D\Omega}}\frac{b_1 a_n - a_1 b_n}{\pi R_A a_1^2}\right) C_L \tag{43}$$

Maintaining this optimum proportionality between wing twist and lift coefficient results in $A_n = 0$ for $n > 1$. Thus, for such twist-optimized wings, using Eq. (43) in Eq. (23) results in

$$\tilde{C}_L(\theta) = \frac{4b}{c(\theta)} A_1 \sin(\theta) = C_L \frac{4b \sin(\theta)}{\pi R_A c(\theta)} \tag{44}$$

The maximum in this section lift distribution is obtained from

$$\frac{\mathrm{d}\tilde{C}_L}{\mathrm{d}\theta} = C_L \frac{4b}{\pi R_A}\left[\frac{\cos(\theta)c(\theta) - \sin(\theta)\,\mathrm{d}c/\,\mathrm{d}\theta}{c^2(\theta)}\right] = 0$$

or

$$\cos(\theta)c(\theta) = \sin(\theta)\frac{\mathrm{d}c}{\mathrm{d}\theta} \tag{45}$$

For the special case of wings with linear taper,

$$c(\theta) = \frac{2b}{R_A(1 + R_T)}[1 - (1 - R_T)|\cos\theta|] \tag{46}$$

Using Eq. (46) in Eqs. (44) and (45), we find that, for unswept wings with linear taper and the twist optimized to produce minimum induced drag, the ratio of the total wing lift coefficient to the maximum section lift coefficient is independent of operating conditions and given by

$$\frac{C_L}{\tilde{C}_{L_{\max}}} = \frac{\pi \sin(\theta_{\max})}{2(1 + R_T)} \tag{47}$$

where

$$\theta_{\max} = \cos^{-1}(1 - R_T) \tag{48}$$

Results obtained from Eqs. (47) and (48) are plotted in Fig. 8.

Effect of Wing Sweep

When Eq. (38) and Figs. 3–7 are used to estimate the wing lift coefficient that corresponds to a given maximum airfoil section lift coefficient, the result applies only to wings without sweep. As a lifting wing of any planform is swept back, the lift near the root of each semispan is reduced as a result of the downwash induced by the

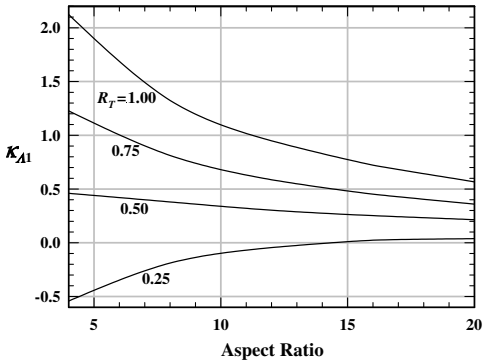

Fig. 9 Sweep coefficient $\kappa_{\Lambda 1}$ to be used in Eq. (50) for wings with linear taper.

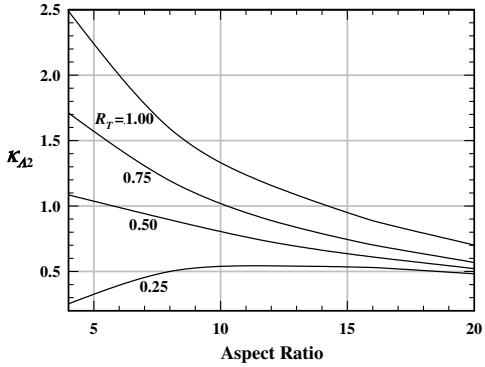

Fig. 10 Sweep coefficient $\kappa_{\Lambda 2}$ to be used in Eq. (50) for wings with linear taper.

bound vorticity generated on the opposite semispan. This tends to move the point of maximum section lift outboard. For wings with significant taper, this outboard shift causes the point of maximum section lift to occur at an airfoil section having a smaller section chord length, which increases the maximum airfoil section lift coefficient that is produced for a given wing lift coefficient.

To account for this effect of wing sweep, results predicted from Eq. (38) can be multiplied by a sweep correction factor, according to the relation

$$C_L = \left(\frac{C_L}{\tilde{C}_{L_{\max}}}\right)_{\substack{\Omega=0\\ \Lambda=0}} \kappa_{L\Lambda}(\tilde{C}_{L_{\max}} - \kappa_{L\Omega} C_{L,\alpha}\Omega) \tag{49}$$

where the sweep correction factor $\kappa_{L\Lambda}$ depends on the quarter-chord sweep angle and wing planform. Because the series solution to Prandtl's lifting-line equation applies only to unswept wings, a numerical solution is required to evaluate $\kappa_{L\Lambda}$. For wings with linear taper, results obtained from the numerical lifting-line method of Phillips and Snyder [40] correlate well with the approximation

$$\kappa_{L\Lambda} \cong 1 + \kappa_{\Lambda 1}\Lambda - \kappa_{\Lambda 2}\Lambda^{1.2} \tag{50}$$

where Λ is in radians and the coefficients $\kappa_{\Lambda 1}$ and $\kappa_{\Lambda 2}$ depend on aspect ratio and taper ratio, as shown in Figs. 9 and 10, respectively.

The approximate correlation for $\kappa_{L\Lambda}$, which is given by Eq. (50), agrees closely with results obtained from numerical lifting-line computations for sweepback angles less than about 35 deg, taper ratios between 0.25 and 1.0, and aspect ratios between about 4.0 and 20. For example, Fig. 11 shows this comparison for four different wing planforms that all have an aspect ratio of 8. Figure 12 shows lifting-line predictions for the spanwise coordinate of the wing section that supports the maximum airfoil section lift coefficient as a function of the quarter-chord sweep angle for the same four wing planforms.

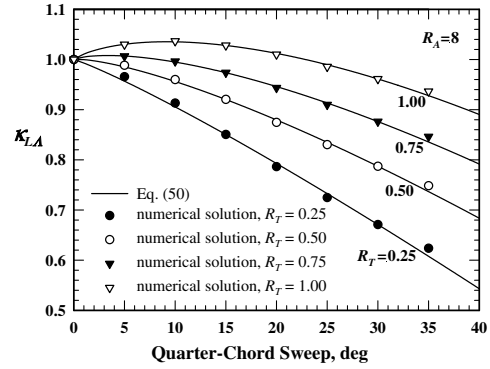

Fig. 11 Comparison between the approximate results for $\kappa_{L\Lambda}$, as predicted from Eq. (50) and those obtained from numerical lifting-line computations.

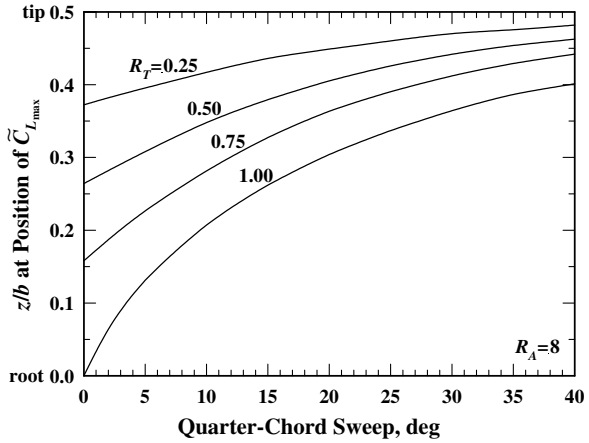

Fig. 12 Spanwise coordinate of the wing section that supports the maximum airfoil section lift coefficient as predicted from numerical lifting-line computations.

Maximum Wing Lift Coefficient

The reader should note that using the maximum airfoil section lift coefficient in Eq. (49) will give an estimate for the wing lift coefficient at the onset of airfoil section stall. At higher angles of attack, separated flow will exist over some sections of the wing and drag will be substantially increased. However, the lift coefficient predicted from Eq. (49) is not exactly the maximum wing lift coefficient. Viscous interactions between adjacent sections of the wing can initiate flow separation at slightly lower angles of attack than predicted by Eq. (49). Furthermore, as the angle of attack is increased somewhat beyond that which produces the onset of airfoil section stall, the section lift coefficient on the stalled section of the wing will decrease. However, the section lift coefficient on the unstalled sections of the wing will continue to increase with angle of attack until the maximum section lift coefficient is also reached on these sections. Thus, the maximum wing lift coefficient could differ slightly from that predicted by Eq. (49). To account for these effects, results predicted from Eq. (49) can be modified by including a stall correction factor:

$$C_{L_{\max}} = \left(\frac{C_L}{\tilde{C}_{L_{\max}}}\right)_{\substack{\Omega=0\\ \Lambda=0}} \kappa_{Ls}\kappa_{L\Lambda}(\tilde{C}_{L_{\max}} - \kappa_{L\Omega} C_{L,\alpha}\Omega) \tag{51}$$

For wings with linear taper and linear twist, results obtained from computational fluid dynamics (CFD) correlate well with the approximate relation [41]:

$$\kappa_{Ls} = 1 + (0.0042R_A - 0.068)(1 + 2.3C_{L,\alpha}\Omega/\tilde{C}_{L_{\max}}) \tag{52}$$

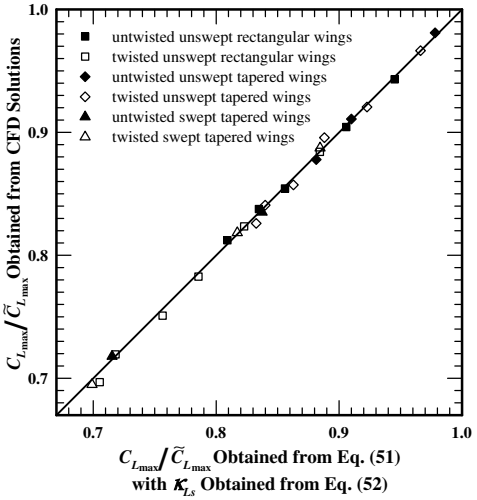

Fig. 13 Comparison between maximum lift coefficients obtained from grid-resolved CFD solutions and those obtained from Eq. (51).

When the correlation expressed in Eq. (52) is used to estimate the stall factor, and the result is used in Eq. (51) together with the lifting-line results presented here, the maximum wing lift coefficient can be estimated from knowledge of the wing geometry and the maximum airfoil section lift coefficient. For example, Fig. 13 shows a comparison between results obtained from Eq. (51) and results obtained from grid-resolved CFD solutions for 25 different wing geometries. These wings had aspect ratios ranging from 4 to 20, taper ratios from 0.5 to 1.0, quarter-chord sweep angles from 0 to 30 deg, and linear geometric washout ranging from 0 to 8 deg. For this range of wing parameters, the ratio $C_{L_{\max}}/\tilde{C}_{L_{\max}}$ varied from about 0.70 to 0.98, with high-aspect-ratio tapered wings producing the highest values. The lowest values of $C_{L_{\max}}/\tilde{C}_{L_{\max}}$ occurred for low-aspect-ratio wings with a high degree of washout and/or sweep. In all cases, Eq. (51) agrees with the results obtained from the CFD solutions to within about $\pm 1\%$.

Designing a Twist Distribution for a Specified Lift Distribution

In addition to predicting the section lift coefficient distribution for a wing of known planform and twist distribution, Eq. (26) can also be used to design a twist distribution for a wing of any planform, which will produce any desired section lift coefficient distribution. If $\tilde{C}_{Ld}(\theta)$ is the design section lift coefficient distribution that is to be produced over the span of an unswept wing having the planform chord length distribution $c(\theta)$, Eq. (26) requires

$$\frac{\tilde{C}_{Ld}(\theta)}{C_L} = \frac{\Omega}{C_L}\sum_{n=1}^{\infty} 4\left(\frac{b_1 a_n}{a_1} - b_n\right)\frac{\sin(n\theta)}{c(\theta)/b} + \sum_{n=1}^{\infty}\frac{4a_n}{\pi R_A a_1}\frac{\sin(n\theta)}{c(\theta)/b}$$

or

$$\sum_{n=1}^{\infty}\frac{4}{\pi R_A a_1}\left[a_n + \left(\frac{b_1 a_n}{a_1} - b_n\right)\frac{C_{L,\alpha}\Omega}{C_L}\right]\sin(n\theta) = \frac{c(\theta)\tilde{C}_{Ld}(\theta)}{bC_L} \tag{53}$$

A Fourier series expansion of any function $f(\theta)$ can be expressed over the domain $\theta = 0$ to π as

$$f(\theta) = \sum_{n=1}^{\infty} B_n \sin(n\theta) \quad \text{with} \quad B_n \equiv \frac{2}{\pi}\int_{\theta=0}^{\pi} f(\theta)\sin(n\theta)\,\mathrm{d}\theta \tag{54}$$

Comparing Eqs. (53) and (54), we see that

$$\frac{4}{\pi R_A a_1}\left[a_n + \left(\frac{b_1 a_n}{a_1} - b_n\right)\frac{C_{L,\alpha}\Omega}{C_L}\right] = \frac{2}{\pi}\int_{\theta=0}^{\pi}\frac{c(\theta)\tilde{C}_{Ld}(\theta)}{bC_L}\sin(n\theta)\,\mathrm{d}\theta \equiv q_n \tag{55}$$

which requires

$$\frac{4}{\pi R_A} = \frac{2}{\pi}\int_{\theta=0}^{\pi}\frac{c(\theta)\tilde{C}_{Ld}(\theta)}{bC_L}\sin(\theta)\,\mathrm{d}\theta = \frac{4}{\pi b^2 C_L}\int_{z=-b/2}^{b/2} c(z)\tilde{C}_{Ld}(z)\,\mathrm{d}z = q_1 \tag{56}$$

and

$$b_n = \left(a_n - \frac{\pi R_A a_1 q_n}{4}\right)\frac{C_L}{C_{L,\alpha}\Omega} + \frac{b_1 a_n}{a_1}, \quad \text{for } n > 1 \tag{57}$$

Equation (56) is satisfied by the definitions of wing lift coefficient and aspect ratio. Equation (57) relates the Fourier coefficients b_n for $n > 1$ to the Fourier coefficients a_n, q_n, and b_1.

The twist distribution function $\omega(\theta)$ is related to the Fourier coefficients b_n through Eq. (13) [29]. Using Eq. (57) in Eq. (13) yields

$$\omega(\theta) = b_1\left[\frac{4b}{\tilde{C}_{L,\alpha}c(\theta)} + \frac{1}{\sin(\theta)}\right]\sin(\theta) + \sum_{n=2}^{\infty}\left[\left(a_n - \frac{\pi R_A a_1 q_n}{4}\right)\frac{C_L}{C_{L,\alpha}\Omega} + \frac{b_1 a_n}{a_1}\right]\times\left[\frac{4b}{\tilde{C}_{L,\alpha}c(\theta)} + \frac{n}{\sin(\theta)}\right]\sin(n\theta)$$

which is easily rearranged as

$$\omega(\theta) = b_1\left[\frac{4b\sin(\theta)}{\tilde{C}_{L,\alpha}c(\theta)} + 1\right] - \left[\left(a_1 - \frac{\pi R_A a_1 q_1}{4}\right)\frac{C_L}{C_{L,\alpha}\Omega} + b_1\right]\left[\frac{4b\sin(\theta)}{\tilde{C}_{L,\alpha}c(\theta)} + 1\right] + \sum_{n=1}^{\infty}\left[\left(a_n - \frac{\pi R_A a_1 q_n}{4}\right)\frac{C_L}{C_{L,\alpha}\Omega} + \frac{b_1 a_n}{a_1}\right]\left[\frac{4b}{\tilde{C}_{L,\alpha}c(\theta)} + \frac{n}{\sin(\theta)}\right]\sin(n\theta)$$

In view of Eq. (56), $a_1 - \pi R_A a_1 q_1/4 = 0$ and we have

$$\omega(\theta) = \sum_{n=1}^{\infty}\left[\left(a_n - \frac{\pi R_A a_1 q_n}{4}\right)\frac{C_L}{C_{L,\alpha}\Omega} + \frac{b_1 a_n}{a_1}\right]\times\left[\frac{4b}{\tilde{C}_{L,\alpha}c(\theta)} + \frac{n}{\sin(\theta)}\right]\sin(n\theta)$$

which can be further rearranged to give

$$\omega(\theta) = \left(\frac{C_L}{C_{L,\alpha}\Omega} + \frac{b_1}{a_1}\right)\sum_{n=1}^{\infty} a_n\left[\frac{4b}{\tilde{C}_{L,\alpha}c(\theta)} + \frac{n}{\sin(\theta)}\right]\sin(n\theta) - \frac{\pi R_A a_1}{4}\frac{C_L}{C_{L,\alpha}\Omega}\sum_{n=1}^{\infty} q_n\left[\frac{4b}{\tilde{C}_{L,\alpha}c(\theta)} + \frac{n}{\sin(\theta)}\right]\sin(n\theta)$$

However, the Fourier coefficients a_n must satisfy Eq. (12), and the wing lift slope is given by Eq. (16). Thus, the twist distribution function can be written as

$$\omega(\theta) = \left(\frac{C_L}{\pi R_A a_1\Omega} + \frac{b_1}{a_1}\right) - \frac{C_L}{\Omega}\sum_{n=1}^{\infty}\frac{q_n}{4}\left[\frac{4b}{\tilde{C}_{L,\alpha}c(\theta)} + \frac{n}{\sin(\theta)}\right]\sin(n\theta) \tag{58}$$

The twist distribution function $\omega(\theta)$ is defined to be the total twist distribution, relative to the wing root, divided by the reference twist Ω, which is defined to be the twist at some reference position, usually the wingtips. For a given wing planform, all of the Fourier coefficients a_n and q_n are known from Eqs. (12) and (55), respectively. Thus, the only unknown Fourier coefficient in Eq. (58) is b_1. Because the twist is defined relative to the wing root, Eq. (58) evaluated at the wing root requires

$$\omega(\pi/2) = \left(\frac{C_L}{\pi R_A a_1 \Omega} + \frac{b_1}{a_1}\right) - \frac{C_L}{\Omega}\sum_{n=1}^{\infty}\frac{q_n}{4}\left(\frac{4b}{\tilde{C}_{L,\alpha}c(\pi/2)} + \frac{n}{\sin(\pi/2)}\right)\sin(n\pi/2) = 0$$

or, after rearranging,

$$\frac{b_1}{a_1} = \frac{C_L}{\Omega}\sum_{n=1}^{\infty}\frac{q_n}{4}\left(\frac{4b}{\tilde{C}_{L,\alpha}c(\pi/2)} + \frac{n}{\sin(\pi/2)}\right)\sin(n\pi/2) - \frac{C_L}{\pi R_A a_1 \Omega} \tag{59}$$

Selecting the usual convention of defining the reference twist Ω to be that at the wingtips, Eq. (58) evaluated at the wingtip requires

$$\omega(0) = 1 \tag{60}$$

Combining Eqs. (58–60) with Eq. (55), we find that the twist distribution required to produce a specified section lift distribution across the span of an unswept wing of arbitrary planform is proportional to the wing lift coefficient and may be expressed as

$$\omega(\theta) = \frac{F(\pi/2) - F(\theta)}{F(\pi/2) - F(0)} \tag{61}$$

where

$$F(\theta) \equiv \sum_{n=1}^{\infty} w_n\left[\frac{4b}{\tilde{C}_{L,\alpha}c(\theta)} + \frac{n}{\sin(\theta)}\right]\sin(n\theta) \tag{62}$$

$$w_n \equiv \frac{1}{2\pi}\int_{\theta=0}^{\pi}\frac{c(\theta)\tilde{C}_{Ld}(\theta)}{bC_L}\sin(n\theta)\,\mathrm{d}\theta \tag{63}$$

and the total required twist at the wingtips is given by

$$\Omega = [F(\pi/2) - F(0)]C_L \tag{64}$$

As a simple example of how Eqs. (61–64) can be applied, consider the wing twist distribution that produces an elliptic lift distribution, which results in minimum induced drag. This requires

$$\frac{c(\theta)\tilde{C}_{Ld}(\theta)}{bC_L} = \frac{4}{\pi R_A}\sin(\theta) \tag{65}$$

Using Eq. (65) in Eq. (63) yields

$$w_n = \frac{2}{\pi^2 R_A}\int_{\theta=0}^{\pi}\sin(\theta)\sin(n\theta)\,\mathrm{d}\theta = \begin{cases} 1/(\pi R_A), & n = 1 \\ 0, & n \neq 1 \end{cases} \tag{66}$$

Applying Eq. (66) to Eq. (62) and using the result in Eqs. (61) and (64) gives

$$\omega(\theta) = 1 - \frac{\sin(\theta)}{c(\theta)/c_{\text{root}}} \tag{67}$$

and

$$\Omega = \frac{4bC_L}{\pi R_A \tilde{C}_{L,\alpha} c_{\text{root}}} \tag{68}$$

Equation (67) is identical to Eq. (20), which was presented by Phillips [29]. Furthermore, it can be shown that Eq. (68) is numerically equivalent to Eq. (21), also presented by Phillips. For the special case of wings with linear taper, $c_{\text{root}} = 2b/[R_A(1 + R_T)]$ and Eq. (68) becomes

$$\Omega = \frac{2(1 + R_T)C_L}{\pi\tilde{C}_{L,\alpha}} \tag{69}$$

which is the relation presented by Phillips et al. [30].

Although the twist distribution for minimum induced drag that is specified by Eqs. (67) and (68) was developed analytically from Eqs. (61–64), in some cases, it is necessary to evaluate these relations numerically. To develop a useful numerical method for this purpose, we first examine a numerical procedure for evaluating the Fourier coefficients w_n from Eq. (63).

For convenience, we will define the function $f(\theta)$ as

$$f(\theta) \equiv \frac{c(\theta)\tilde{C}_{Ld}(\theta)}{bC_L} \tag{70}$$

If both the wing planform and the design lift distribution are symmetric about the wing root ($\theta = \pi/2$), the numerical procedure can be simplified. Using the definition in Eq. (70) and enforcing such symmetry on Eq. (63) results in

$$\begin{aligned} w_n &\equiv \frac{1}{2\pi}\int_{\theta=0}^{\pi} f(\theta)\sin(n\theta)\,\mathrm{d}\theta \\ &= \begin{cases} 0, & n \text{ even} \\ \dfrac{1}{\pi}\displaystyle\int_{\theta=0}^{\pi/2} f(\theta)\sin(n\theta)\,\mathrm{d}\theta, & n \text{ odd} \end{cases} \end{aligned} \tag{71}$$

For numerical evaluation of the integral in Eq. (71), the domain from $\theta = 0$ to $\theta = \pi/2$ is divided into $M - 1$ increments between M nodes, which are spaced equally in θ, with node 1 at the wingtip ($\theta = 0$) and node M at the root ($\theta = \pi/2$). The function $f(\theta)$ is approximated as being linear over each of these increments, which gives

$$\begin{aligned} &\int_{\theta=0}^{\pi/2} f(\theta)\sin(n\theta)\,\mathrm{d}\theta \\ &\quad\cong \sum_{i=1}^{M-1}\int_{\theta=\theta_i}^{\theta_{i+1}}\left[f_i + \frac{f_{i+1} - f_i}{\delta\theta}(\theta - \theta_i)\right]\sin(n\theta)\,\mathrm{d}\theta \end{aligned} \tag{72}$$

where $\delta\theta = \pi/[2(M-1)]$, $\theta_i = (i-1)\delta\theta$, and $f_i = f(\theta_i)$. After performing the integration and rearranging, we obtain the result

$$\begin{aligned} &\int_{\theta=0}^{\pi/2} f(\theta)\sin(n\theta)\,\mathrm{d}\theta \\ &\quad\cong \left[\frac{\cos(n\theta_1)}{n} + \frac{\sin(n\theta_1) - \sin(n\theta_2)}{n^2\delta\theta}\right]f_1 \\ &\quad + \sum_{i=2}^{M-1}\frac{2\sin(n\theta_i) - \sin(n\theta_{i-1}) - \sin(n\theta_{i+1})}{n^2\delta\theta}f_i \\ &\quad + \left[\frac{-\cos(n\theta_M)}{n} + \frac{\sin(n\theta_M) - \sin(n\theta_{M-1})}{n^2\delta\theta}\right]f_M \end{aligned} \tag{73}$$

This result can be simplified somewhat by recognizing that $\theta_1 = 0$ and $\theta_M = \pi/2$. Thus, applying Eqs. (73) to Eq. (71) results in

$$w_n \cong \begin{cases} 0, & n \text{ even} \\ \sum_{i=1}^{M} W_{ni} f_i, & n \text{ odd} \end{cases} \tag{74}$$

where

$$W_{ni} \equiv \begin{cases} \dfrac{1}{n\pi} - \dfrac{\sin(n\theta_2)}{n^2\pi\delta\theta}, & i = 1 \\ \dfrac{2\sin(n\theta_i) - \sin(n\theta_{i-1}) - \sin(n\theta_{i+1})}{n^2\pi\delta\theta}, & 1 < i < M \\ \dfrac{\sin(n\pi/2) - \sin(n\theta_{M-1})}{n^2\pi\delta\theta}, & i = M \end{cases} \tag{75}$$

Using Eqs. (74) and (75) in Eq. (62) and truncating the infinite series to N of the nonzero odd terms, the function $F(\theta)$ can be numerically approximated as

$$F(\theta) \cong \sum_{i=1}^{M} G_i(\theta) f_i \tag{76}$$

where

$$G_i(\theta) \equiv \sum_{k=1}^{N} W_{ki} g_k(\theta) \tag{77}$$

$$W_{ki} \equiv \begin{cases} \dfrac{1}{(2k-1)\pi} - \dfrac{\sin(\phi_{k2})}{\delta_k}, & i = 1 \\ \dfrac{2\sin(\phi_{ki}) - \sin(\phi_{ki-1}) - \sin(\phi_{ki+1})}{\delta_k}, & 1 < i < M \\ \dfrac{(-1)^{k+1} - \sin(\phi_{kM-1})}{\delta_k}, & i = M \end{cases} \tag{78}$$

$$\phi_{ki} \equiv (2k-1)\theta_i \tag{79}$$

$$\theta_i \equiv \frac{(i-1)\pi}{2(M-1)} \tag{80}$$

$$\delta_k \equiv \frac{(2k-1)^2\pi^2}{2(M-1)} \tag{81}$$

$$f_i \equiv \frac{c(\theta_i)\tilde{C}_{Ld}(\theta_i)}{bC_L} \tag{82}$$

$$g_k(\theta) \equiv \left[\frac{4b}{\tilde{C}_{L,\alpha} c(\theta)} + \frac{2k-1}{\sin(\theta)}\right] \sin[(2k-1)\theta] \tag{83}$$

The reader should notice that evaluating $g_k(\theta)$ from Eq. (83) is numerically indeterminate at the wingtips ($\theta = 0$ and $\theta = \pi$). However, from l'Hôspital's rule, we have

$$\left(\frac{\sin(n\theta)}{\sin(\theta)}\right)_{\theta\to 0} = \left(\frac{n\cos(n\theta)}{\cos(\theta)}\right)_{\theta\to 0} = n$$

and

$$\left(\frac{\sin(n\theta)}{\sin(\theta)}\right)_{\theta\to \pi} = \left(\frac{n\cos(n\theta)}{\cos(\theta)}\right)_{\theta\to \pi} = (-1)^{n+1} n$$

for any integer value of n. Thus, for numerical evaluation of Eq. (77) at the wing tips, we use

$$g_k(0) = g_k(\pi) = (2k-1)^2 \tag{84}$$

Using Eqs. (76–84) to evaluate $F(\theta)$ numerically, the result can be applied to Eqs. (61) and (64) to obtain the twist distribution required to produce any desired lift distribution on a wing of any given planform.

Maximizing Lift with Wing Twist

In the preceding section, Eqs. (61–64) were used to obtain the twist distribution that results in minimum induced drag. However, minimizing drag is not necessarily the highest priority in all mission phases. For example, during takeoff and landing, it can be more important to maximize the lift coefficient. If the maximum attainable airfoil section lift coefficient is constant across the span of the wing, to achieve the absolute maximum in the wing lift coefficient that is attained before the onset of stall, the section lift coefficient would need to be uniform over the wingspan. It is mathematically quite simple to apply Eqs. (61–64) to obtain the twist distribution for an unswept wing of any planform, which produces a uniform section lift coefficient, according to Eq. (26). For example, using $\tilde{C}_{Ld}(\theta)/C_L = 1$ for a wing with linear taper in Eqs. (61–64) results in

$$\frac{c(\theta)}{b} = \frac{2[1 - (1 - R_T)|\cos(\theta)|]}{R_A(1 + R_T)} \tag{85}$$

$$w_n = \begin{cases} \dfrac{1}{\pi R_A}, & n = 1 \\ 0, & n \text{ even} \\ \dfrac{c(\pi/2)}{\pi b}\left\{\dfrac{1}{n} - \dfrac{1 - R_T}{n^2 - 1}[n + (-1)^{(n+1)/2}]\right\}, & n > 1 \text{ odd} \end{cases} \tag{86}$$

$$\begin{aligned} \frac{\Omega\omega(\theta)}{C_L} = F(\pi/2) - F(\theta) = {} & \frac{4}{\pi R_A \tilde{C}_{L,\alpha}}\left\{\frac{b}{c(\pi/2)} - \frac{b}{c(\theta)}\sin(\theta)\right\} \\ & - \sum_{i=2}^{\infty}(-1)^i w_{2i-1}\left[\frac{4b}{\tilde{C}_{L,\alpha} c(\pi/2)} + 2i - 1\right] \\ & - \sum_{i=2}^{\infty} w_{2i-1}\left\{\frac{4b}{\tilde{C}_{L,\alpha} c(\theta)} + \frac{2i-1}{\sin(\theta)}\right\}\sin[(2i-1)\theta] \end{aligned} \tag{87}$$

$$\begin{aligned} \frac{\Omega}{C_L} = F(\pi/2) - F(0) = {} & \frac{4b}{\pi R_A \tilde{C}_{L,\alpha} c(\pi/2)} \\ & - \sum_{i=2}^{\infty} w_{2i-1}\left\{(-1)^i\left[\frac{4b}{\tilde{C}_{L,\alpha} c(\pi/2)} + 2i - 1\right] + (2i-1)^2\right\} \end{aligned} \tag{88}$$

However, this twist distribution is not practical, because maintaining a uniform section lift coefficient over the entire span of the wing, from the root to the wingtips, requires too much twist in the region very close to the wingtips.

It is mathematically possible to use Eqs. (61–64) to find the twist distribution for an unswept wing of any conceivable planform, which will produce any imaginable lift distribution from Eq. (26). This does not mean that the twist distribution so determined could actually be implemented on a practical wing. To assure that the wing design is practical, some constraint must be placed on the wing twist. To demonstrate how this is accomplished, we turn to the numerical formulation defined by Eqs. (76–84).

Defining $F_j \equiv F(\theta_j)$, $G_{ij} \equiv G_i(\theta_j)$, and $g_{kj} \equiv g_k(\theta_j)$, Eqs. (76), (77), and (83) are used to create an M by M system of linear equations. Setting $N = M$, this gives

$$F_j = \sum_{i=1}^{M} G_{ij} f_i, \qquad 1 \le j \le M \tag{89}$$

where

$$G_{ij} \equiv \sum_{k=1}^{M} W_{ki} g_{kj} \tag{90}$$

and

$$g_{kj} \equiv \begin{cases} (2k-1)^2, & j = 1 \\ \left[\dfrac{4b}{\tilde{C}_{L,\alpha} c(\theta_j)} + \dfrac{2k-1}{\sin(\theta_j)}\right]\sin(\phi_{kj}), & j > 1 \end{cases} \tag{91}$$

This linear system can be rearranged as

$$\begin{aligned} \sum_{i=1}^{m_t-1} G_{ij} f_i - F_j &= -\sum_{i=m_t}^{M} G_{ij} f_i, \quad j < m_t \\ -\sum_{i=1}^{m_t-1} G_{ij} f_i + F_j &= \sum_{i=m_t}^{M} G_{ij} f_i, \quad j \geq m_t \end{aligned} \tag{92}$$

The system of equations obtained from Eq. (92) can be solved for the case in which the wing twist is specified over part of the wing and the section lift coefficient is specified over the remainder of the wing. To avoid excessive twist near the wingtips, we specify the twist over some wingtip transition region extending from the wingtip at $\theta = 0$ to some transition point at $\theta = \theta_{m_t}$. The section lift coefficient is specified over the remainder of the wing from $\theta = \theta_{m_t}$ to the wing root at $\theta = \pi/2$.

For example, to specify a section of constant twist from the wingtip to θ_{m_t}, one would use

$$F_j = F_{m_t}, \qquad j < m_t \tag{93}$$

Using Eq. (93) in Eq. (92) provides a linear system of M equations in M unknowns. These unknowns are the values of the lift-dependent function f_i over the tip region ($1 \leq i \leq m_t - 1$) and the values of the twist-dependent function F_i over the remainder of the wing ($m_t \leq i \leq M$). Once all M of the F_i values are known from the solution to Eqs. (92) and (93), the required twist distribution for the wing can be determined from Eqs. (61) and (64).

Any twist distribution could be used for the tip region in place of Eq. (93). All that is required is that the values of F_i throughout the tip region must be specified in terms of the remaining unknowns. To specify linear twist from the wingtip to θ_{m_t}, we apply the definition of θ from Eq. (3), which results in

$$\begin{aligned} F_j = &\frac{\cos(\theta_{m_t+1}) - \cos(\theta_j)}{\cos(\theta_{m_t+1}) - \cos(\theta_{m_t})} F_{m_t} \\ &+ \frac{\cos(\theta_j) - \cos(\theta_{m_t})}{\cos(\theta_{m_t+1}) - \cos(\theta_{m_t})} F_{m_t+1}, \qquad j < m_t \end{aligned} \tag{94}$$

Similarly, a parabolic twist distribution with zero slope at the wingtip can be specified for the tip region by using

$$F_j = (1 + C_j) F_{m_t} - C_j F_{m_t+1}, \qquad j < m_t \tag{95}$$

where

$$C_j \equiv \frac{[2 - \cos(\theta_j) - \cos(\theta_{m_t})][\cos(\theta_j) - \cos(\theta_{m_t})]}{2[1 - \cos(\theta_{m_t})][\cos(\theta_{m_t}) - \cos(\theta_{m_t+1})]} \tag{96}$$

The exact form of the twist distribution used for the wingtip region is not critical and can be chosen on the basis of what is mechanically achievable. For example, Fig. 14 shows the twist distributions for a tapered wing that are obtained from Eq. (92) using the twist specified by Eqs. (93–95) over a wingtip region defined to be the outboard 5% of the wingspan. Over the remaining 90% of the span, the twist is that required to produce a constant section lift coefficient of 1.6. For comparison, Fig. 14 also shows the twist distribution required to minimize the induced drag at the wing lift coefficient that results in a maximum section lift coefficient of 1.6. Although the twist distributions produced from Eqs. (93–95) differ substantially in the wingtip region, the lift coefficient distributions obtained from these three twist distributions are very similar. Figure 15 shows the lift coefficient distributions obtained using Eqs. (93–95) compared with the lift coefficient distributions for an untwisted wing and a wing with the twist distribution required to minimize induced drag. In all cases, the angle of attack was set to give a maximum airfoil section lift coefficient of 1.6. The total wing lift coefficients obtained using Eqs. (93–95) are 1.577, 1.584, and 1.583, respectively, whereas that obtained with no twist is 1.509 and that obtained with the twist required to minimize induced drag is 1.451.

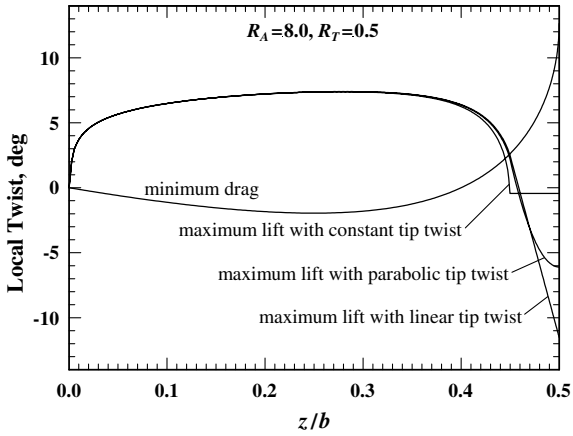

Fig. 14 Wing twist distributions for approximating maximum lift, as obtained from Eq. (92) using the wingtip twist distributions specified by Eqs. (93–95) over a wingtip region defined to be the outboard 5% of the wingspan.

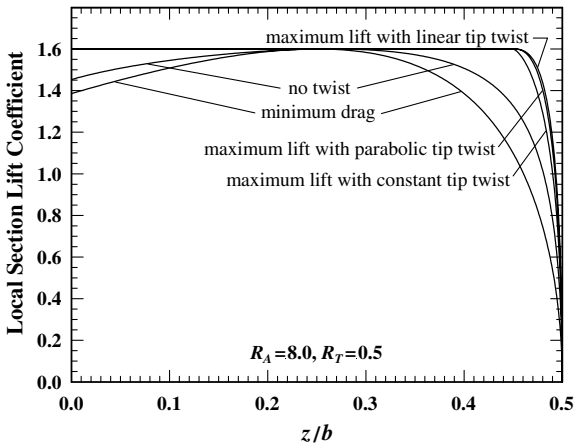

Fig. 15 Section lift coefficient distributions for approximating maximum lift, as obtained from Eq. (92) using the wingtip twist distributions specified by Eqs. (93–95) over a wingtip region defined to be the outboard 5% of the wingspan.

Although the exact form of the twist distribution used for the wingtip region does not greatly affect the net wing lift coefficient that is attained for a given maximum section lift coefficient, the fraction of the total semispan that is included in the wingtip region has a greater effect. As the transition point θ_{m_t} is moved inboard, the magnitude of the twist required at the wingtips is reduced, but the wing lift coefficient that is attained for a given maximum section lift coefficient is also reduced. For example, Fig. 16 shows how the total wing lift coefficient (solid lines) and the total amount of twist required at the wingtips (dashed lines) varies with the position of the wingtip transition point for the same wing planform and maximum section lift coefficient as those used for Figs. 14 and 15.

From Fig. 16, it can be seen that, as the wingtip transition region is reduced in size to increase the fraction of the wingspan that carries a constant section lift coefficient, the magnitude of the twist required in the wingtip region increases. As the size of the wingtip transition region is reduced below about 5% of the wingspan, the required wingtip twist increases very rapidly and becomes larger than that which could be implemented in a practical wing design. Thus, a wingtip transition region comprising about 5% of the wingspan appears to be a good compromise between maximizing the wing lift coefficient and minimizing the required wingtip twist.

Conclusions

Results presented here allow one to estimate the maximum wing lift coefficient from known wing geometry and airfoil section

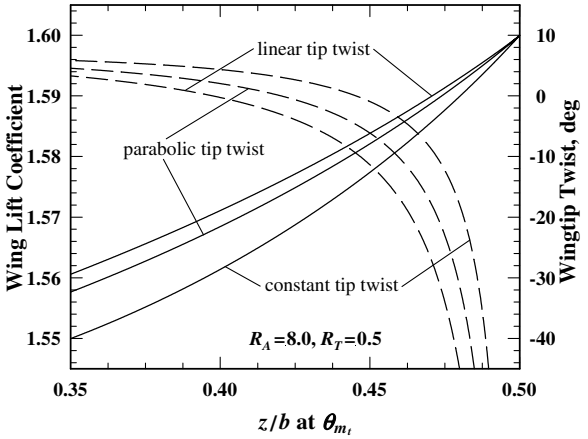

Fig. 16 Variation in wing lift coefficient (solid lines) and wingtip twist (dashed lines) with position of wingtip transition point, as obtained from Eq. (92) using the wingtip twist distributions specified by Eqs. (93–95).

properties. For unswept wings with linear taper and no twist, the ratio of the wing lift coefficient to the maximum airfoil section lift coefficient at the onset of wing stall can be obtained from Fig. 3. This result can be adjusted to estimate the maximum wing lift coefficient for wings with twist and/or sweep by applying Eq. (51). The twist factor in Eq. (51) can be obtained from Figs. 5 and 6, or 7. The sweep factor is evaluated from Eq. (50) using the sweep coefficients obtained from Figs. 9 and 10. The stall factor can be approximated from Eq. (52).

Values for the stall factor estimated from Eq. (52) should be used with caution, because this relation was obtained in [41] by correlating results obtained from CFD computations at a single Reynolds number of 3.0×10^6. Although the CFD results presented in [41] were shown to be grid-resolved and in good agreement with limited experimental data, additional experimental results are needed to fully validate Eq. (52). There are two primary concerns with this correlation. First, CFD computations are not known for being particularly accurate in the region of stall. Second, maximum lift coefficients are known to be a function of Reynolds number. Nevertheless, Eq. (52) was obtained by using CFD computations to evaluate the ratio of 3-D maximum wing lift coefficients to the corresponding 2-D maximum airfoil section lift coefficient. Because small errors in the CFD computations and Reynolds number dependencies should affect the 2-D and 3-D results in a similar manner, these factors should not greatly affect the ratio $C_{L_{\max}}/\tilde{C}_{L_{\max}}$. Furthermore, results presented in [41] show that the correction obtained by using the stall factor predicted from Eq. (52) is less than 10%. Thus, a reasonable first approximation for the maximum wing lift coefficient could be obtained from the results presented here, by neglecting the stall factor completely (i.e., using $\kappa_{L_s} = 1.0$).

In addition to predicting the section lift coefficient distribution for a wing of known planform with a known twist distribution, the lifting-line solution presented here can be used to predict the twist distribution for a wing of any planform, which will produce any desired section lift coefficient distribution along the span of the wing. It was shown that this solution can be used to predict the twist distribution required to minimize induced drag. A method was also presented here that uses this lifting-line solution to predict the twist distribution that maximizes the wing lift coefficient for a given maximum airfoil section lift coefficient, while keeping the total amount of required twist at a practical level.

For the maximum lift computations presented here, it was assumed that the maximum attainable airfoil section lift coefficient is constant across the span of the wing. In this case, the maximum wing lift coefficient is achieved with the twist distribution that produces a uniform section lift coefficient across the wingspan. However, the method described here for maximizing the wing lift coefficient with wing twist is not limited to this special case. When trailing-edge flaps are deflected or the wing has some other type of aerodynamic twist, the maximum attainable airfoil section lift coefficient may vary with the spanwise coordinate. Because the present method can be used to solve for the twist distribution that will produce any desired section lift coefficient distribution, the technique can be used to predict the twist distribution that will maximize the wing lift coefficient for any wing geometry.

We have seen here that the twist distribution required to minimize induced drag is typically quite different from that required to maximize the wing lift coefficient. Furthermore, the amount of twist needed to minimize induced drag varies with the wing lift coefficient. Thus, wing twist can be optimized only for a single design operating condition when only fixed twist is employed. On the other hand, if variable twist is implemented using an active feedback control system, wing twist can be varied with operating conditions to maintain minimum induced drag in cruise configuration over a wide range of altitude, gross weight, and airspeed. Furthermore, during takeoff and landing, this same variable-twist control system could be used to maximize the wing lift coefficient, providing lower airspeeds for shorter takeoff/landing distances and greater safety.

References

[1] Prandtl, L., "Tragflügel Theorie," *Nachricten von der Gesellschaft der Wissenschaften zu Göttingen*, Ges-Chäeftliche Mitteilungen, Klasse, Germany, 1918, pp. 451–477.

[2] Prandtl, L., "Applications of Modern Hydrodynamics to Aeronautics," NACA TR-116, June 1921.

[3] Glauert, H., "The Monoplane Aerofoil," *The Elements of Aerofoil and Airscrew Theory*, Cambridge Univ. Press, Cambridge, England, U.K., 1926, pp. 137–155.

[4] Multhopp, H., "Die Berechnung der Auftriebs Verteilung von Tragflugeln," *Luftfahrtforschung*, Vol. 15, No. 14, 1938, pp. 153–169.

[5] Lotz, I., "Berechnung der Auftriebsverteilung Beliebig Geformter Flugel," *Zeitschrift für Flugtechnik und Motorluftschiffahrt*, Vol. 22, No. 7, 1931, pp. 189–195.

[6] Karamcheti, K., "Elements of Finite Wing Theory," *Ideal-Fluid Aerodynamics*, Wiley, New York, 1966, pp. 535–567.

[7] Anderson, J. D., "Incompressible Flow over Finite Wings: Prandtl's Classical Lifting-Line Theory," *Fundamentals of Aerodynamics*, 3rd ed., McGraw–Hill, New York, 2001, pp. 360–387.

[8] Bertin, J. J., "Incompressible Flow About Wings of Finite Span," *Aerodynamics for Engineers*, 4th ed., Prentice–Hall, Upper Saddle River, NJ, 2002, pp. 230–302.

[9] Katz, J., and Plotkin, A., "Finite Wing: The Lifting-Line Model," *Low-Speed Aerodynamics*, 2nd ed., Cambridge Univ. Press, Cambridge, England, U.K., 2001, pp. 167–183.

[10] Kuethe, A. M., and Chow, C. Y., "The Finite Wing," *Foundations of Aerodynamics*, 5th ed., Wiley, New York, 1998, pp. 169–219.

[11] McCormick, B. W., "The Lifting-Line Model," *Aerodynamics, Aeronautics, and Flight Mechanics*, 2nd ed., Wiley, New York, 1995, pp. 112–119.

[12] Phillips, W. F., "Incompressible Flow over Finite Wings," *Mechanics of Flight*, Wiley, Hoboken, NJ, 2004, pp. 42–79.

[13] Glauert, H., and Gates, S. B., "The Characteristics of a Tapered and Twisted Wing with Sweep-Back," Aeronautical Research Council, Reports and Memoranda No. 1226, London, Aug. 1929.

[14] Amstutz, E., "Calculation of Tapered Monoplane Wings," NACA TM-578, Feb. 1930.

[15] Anderson, R. F., "Charts for Determining the Pitching Moment of Tapered Wings with Sweepback and Twist," NACA TN-483, Dec. 1933.

[16] Anderson, R. F., "Determination of the Characteristics of Tapered Wings," NACA TR-572, May 1937.

[17] Datwiler, G., "Calculations of the Effect of Wing Twist on the Air Forces Acting on a Monoplane Wing," NACA TN-520, Mar. 1935.

[18] Cohen, D., "A Method of Determining the Camber and Twist of a Surface to Support a Given Distribution of Lift," NACA TN-855, Aug. 1942.

[19] Falkner, V. M., "The Calculation of Aerodynamic Loading on Surfaces of Any Shape," Aeronautical Research Council, Reports and Memoranda No. 1910, London, Aug. 1943.

[20] DeYoung, J., and Harper, C. W., "Theoretical Symmetric Span Loading at Subsonic Speeds for Wings having Arbitrary Plan Form," NACA TR-921, Dec. 1948.

[21] Stevens, V. I., "Theoretical Basic Span Loading Characteristics of Wings with Arbitrary Sweep, Aspect Ratio and Taper Ratio," NACA TN-1772, Dec. 1948.

[22] Munk, M. M., "On the Distribution of Lift Along the Span of an Airfoil with Displaced Ailerons," NACA TN-195, June 1924.
[23] Munk, M. M., "A New Relation Between the Induced Yawing Moment and the Rolling Moment of an Airfoil in Straight Motion," NACA TR-197, June 1925.
[24] Glauert, H., "Theoretical Relationships for an Airfoil with Hinged Flap," Aeronautical Research Council, Reports and Memoranda No. 1095, London, July 1927.
[25] Hartshorn, A. S., "Theoretical Relationship for a Wing with Unbalanced Ailerons," Aeronautical Research Council, Reports and Memoranda No. 1259, London, Oct. 1929.
[26] Pearson, H. A., "Theoretical Span Loading and Moments of Tapered Wings produced by Aileron Deflection," NACA TN-589, Jan. 1937.
[27] Pearson, H. A., "Span Load Distribution for Tapered Wings with Partial-Span Flaps," NACA TR-585, Nov. 1937.
[28] Pearson, H. A., and Jones, R. T., "Theoretical Stability and Control Characteristics of Wings with Various Amounts of Taper and Twist," NACA TR-635, Apr. 1937.
[29] Phillips, W. F., "Lifting-Line Analysis for Twisted Wings and Washout-Optimized Wings," *Journal of Aircraft*, Vol. 41, No. 1, 2004, pp. 128–136.
[30] Phillips, W. F., Alley, N. R., and Goodrich, W. D., "Lifting-Line Analysis of Roll Control and Variable Twist," *Journal of Aircraft*, Vol. 41, No. 5, 2004, pp. 1169–1176.
[31] Phillips, W. F., Fugal, S. R., and Spall, R. E., "Minimizing Induced Drag with Wing Twist, Computational-Fluid-Dynamics Validation," *Journal of Aircraft*, Vol. 43, No. 2, 2006, pp. 437–444.
[32] Silverstein, A., Katzoff, S., and Hootman, J. A., "Comparative Flight and Full-Scale Wind-Tunnel Measurements of the Maximum Lift of an Airplane," NACA TR-618, Feb. 1938.
[33] Spreiter, J. R., and Steffen, P. J., "Effects of Mach and Reynolds Numbers on Maximum Lift Coefficient," NACA TN-1044, Mar. 1946.
[34] Sweberg, H. H., and Dingeldein, R. C., "Summary of Measurements in Langley Full-Scale Tunnel of Maximum Lift Coefficient and Stalling Characteristics of Airplanes," NACA TR-829, Mar. 1947.
[35] Furlong, G. C., and Fitzpatrick, J. E., "Effects of Mach Number and Reynolds Number on the Maximum Lift Coefficient of a Wing of NACA 230-Series Airfoil Section," NACA TN-1299, May 1947.
[36] Fitzpatrick, J. E., and Schneider, W. C., "Effects of Mach Number Variation Between 0.07 and 0.34 and Reynolds Number Variation Between 0.97×10^6 and 8.10×10^6 on the Maximum Lift Coefficient of a Wing of NACA 64-210 Airfoil Section," NACA TN-2753, Aug. 1952.
[37] Valarezo, W. O., and Chin, V. D., "Method for the Prediction of Wing Maximum Lift," *Journal of Aircraft*, Vol. 31, No. 1, 1994, pp. 103–109.
[38] Patel, M. P., Sowle, Z. H., Corke, T. C., and He, C., "Autonomous Sensing and Control of Wing Stall Using a Smart Plasma Slat," AIAA Paper 2006-1207, Jan. 2006.
[39] Saffman, P. G., "Vortex Force and Bound Vorticity," *Vortex Dynamics*, Cambridge Univ. Press, Cambridge, England, U. K., 1992, pp. 46–48.
[40] Phillips, W. F., and Snyder, D. O., "Modern Adaptation of Prandtl's Classic Lifting-Line Theory," *Journal of Aircraft*, Vol. 37, No. 4, 2000, pp. 662–670.
[41] Alley, N. R., Phillips, W. F., and Spall, R. E., "Predicting Maximum Lift Coefficient for Twisted Wings Using Computational Fluid Dynamics," *Journal of Aircraft*, Vol. 44, No. 3, pp. 898–910; also AIAA Paper 2007-0898, Jan. 2007.